Supplementary Information for *GIR v1.0.0: a generalised impulse-response model for climate uncertainty and future scenario exploration*

Nicholas J. Leach[1], Zebedee Nicholls[2,3], Stuart Jenkins[1], Christopher J. Smith[4], John Lynch[1], Michelle Cain[1], Bill Wu[1], Junichi Tsutsui[5], and Myles R. Allen[1,6]

[1]Department of Physics, Atmospheric Oceanic and Planetary Physics, University of Oxford, United Kingdom.
[2]Australian–German Climate and Energy College, University of Melbourne, Australia.
[3]School of Earth Sciences, University of Melbourne, Australia.
[4]School of Earth and Environment, University of Leeds, Leeds, UK.
[5]Environmental Science Laboratory, Central Research Institute of Electric Power Industry, Abiko-shi, Japan.
[6]Environmental Change Institute, University of Oxford, Oxford, UK.

Correspondence: Nicholas J. Leach (nicholas.leach@stx.ox.ac.uk)

Table 1. Units used in GIR when the default parameter set is used for each gas or aerosol species. Default forcing unit for all species is Wm^{-2}.

Variable	CO_2	CH_4	N_2O	SOx	NOx	BC	OC	NH3	VOC	All other WMGHGs
Emissions	PgC	$TgCH_4$	TgN_2O-N_2	$TgSO_2$	TgN	TgC	TgC	Tg	Tg	Tg
Concentrations	ppm	ppb	ppb	-	-	-	-	-	-	ppb
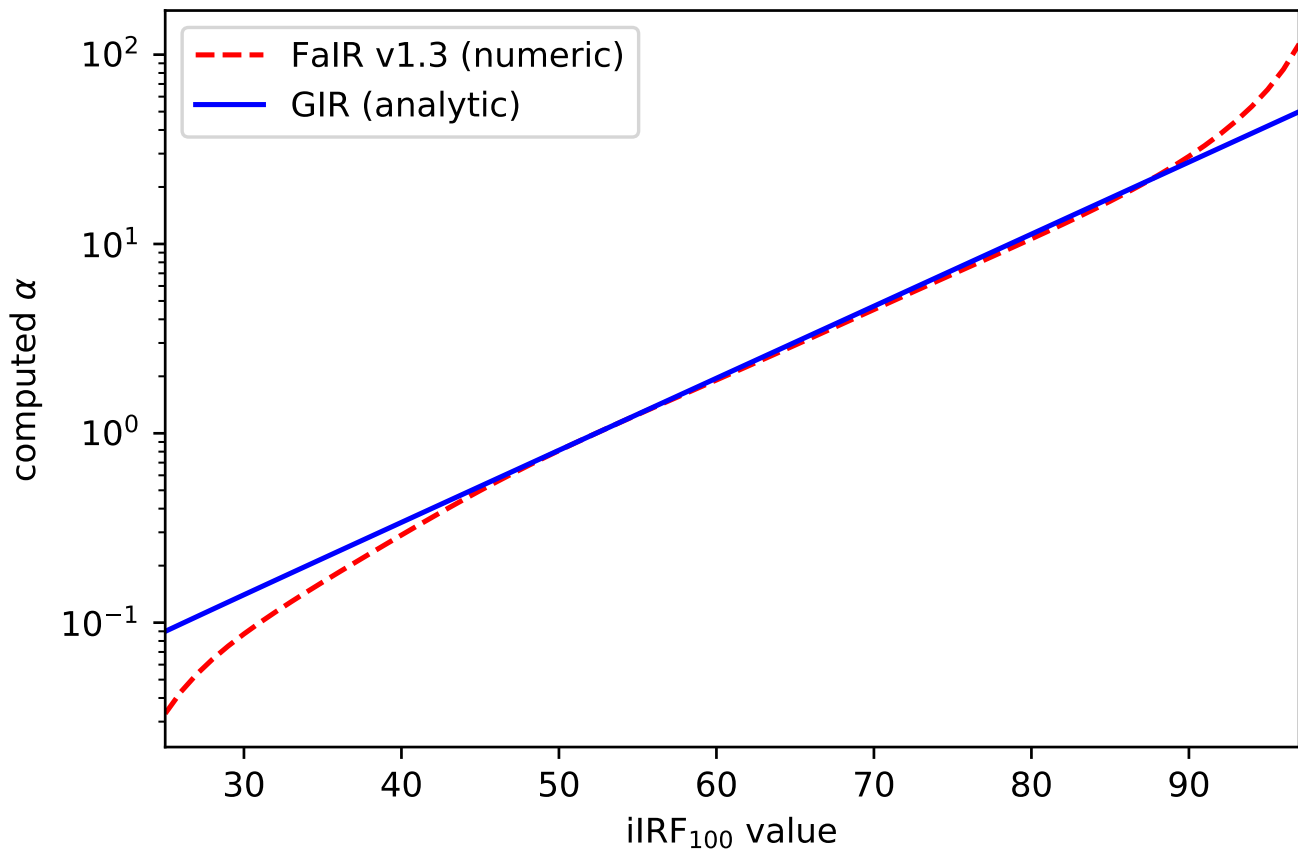
Figure 1. Numerical solution for α in FaIR v1.0 and v1.3 versus analytic solution in GIR. This highlights the reason for the lowered r_0 parameter in GIR compared to FaIR v1.3 (Smith et al., 2017) or v1.0 (Millar et al., 2017), as we see that for pre-industrial α values (0.12 in v1.0 or 0.16 in v1.3), the analytic solution requires a lower iIRF$_{100}$ than the numeric. Despite the marginal difference in shape, we do not find GIR has reduced ability in reproducing historical concentration when compared with FaIR v1.0 or v1.3.
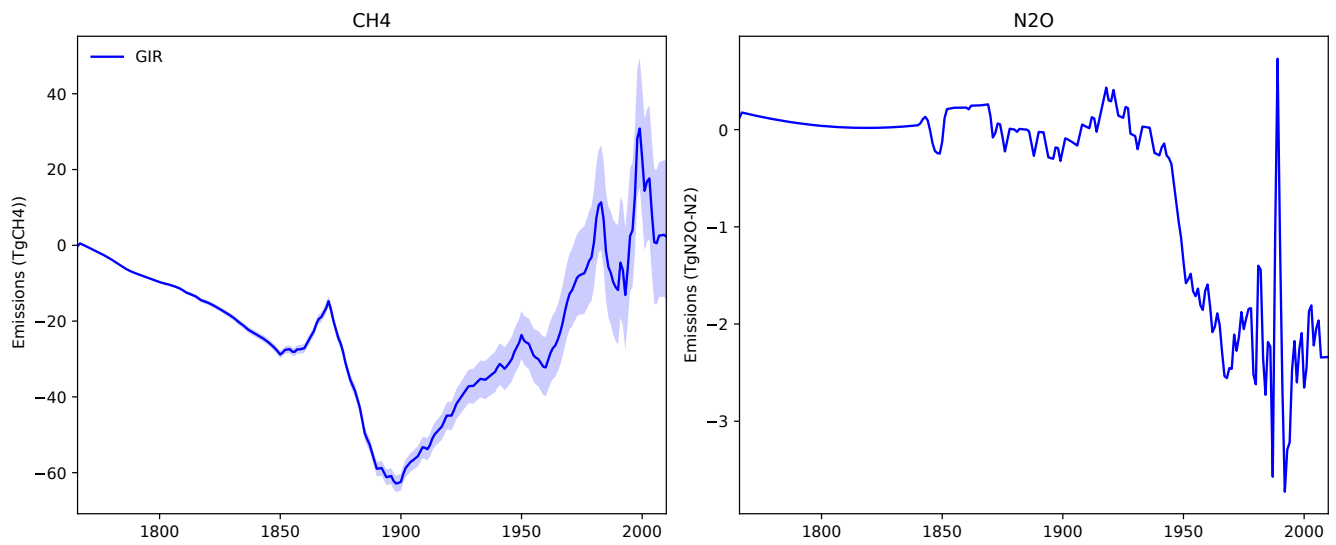
Figure 2. Differences between historical diagnosed emissions in GIR and the RCP database emissions for CH$_4$ and N$_2$O. This displays high similarity to the imposed natural emissions in FaIR v1.3 (Figure 2 from Smith et al. (2017)), demonstrating that CH$_4$ and N$_2$O cycles in GIR and FaIR v1.3 are not systematically different.
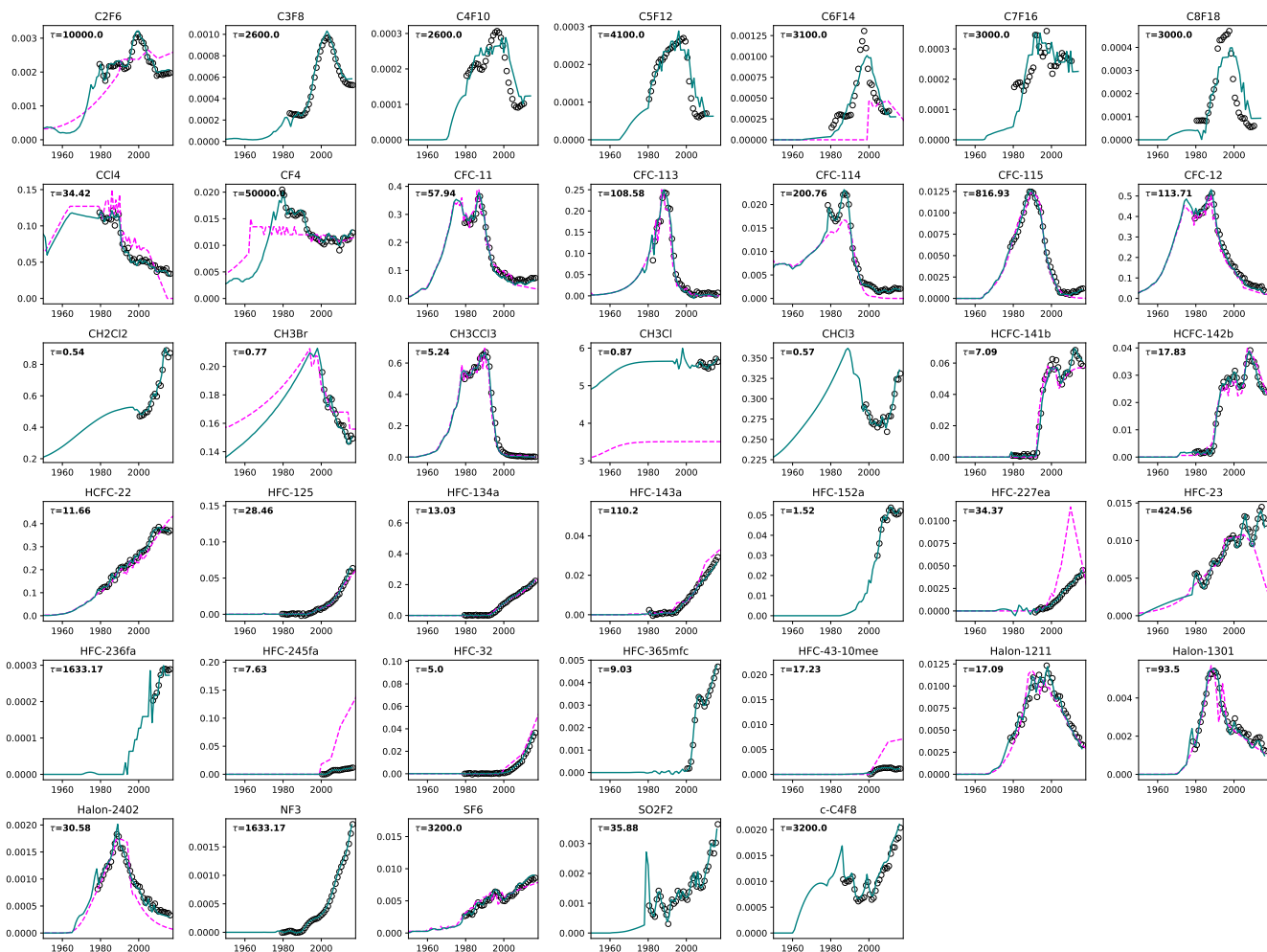
Figure 3. Best-estimate annual emissions (Tg) from a more complex atmospheric model inversion Rigby et al. (2014), GIR inverse emissions and RCP database emissions. Open black circles show inverse emissions from a 12-box model Cunnold et al. (1994); solid green lines show inverse emissions from GIR with tuned parameters and solid pink lines show emissions from the RCP database. Inset text shows the tuned species lifetime.
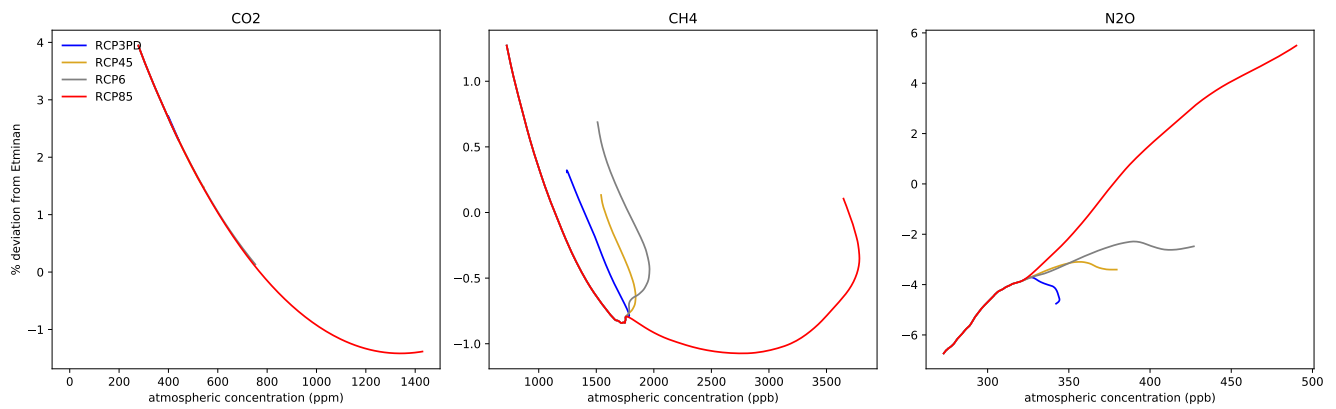
Figure 4. Corresponding deviations of FaIR v2.0 from Etminan et al. (2016) formulae for the RCPs, largely caused by inter-gas interaction terms. These are plotted as % deviations against gas concentration (so absolute deviations are considerably lower at low concentrations than high concentrations).
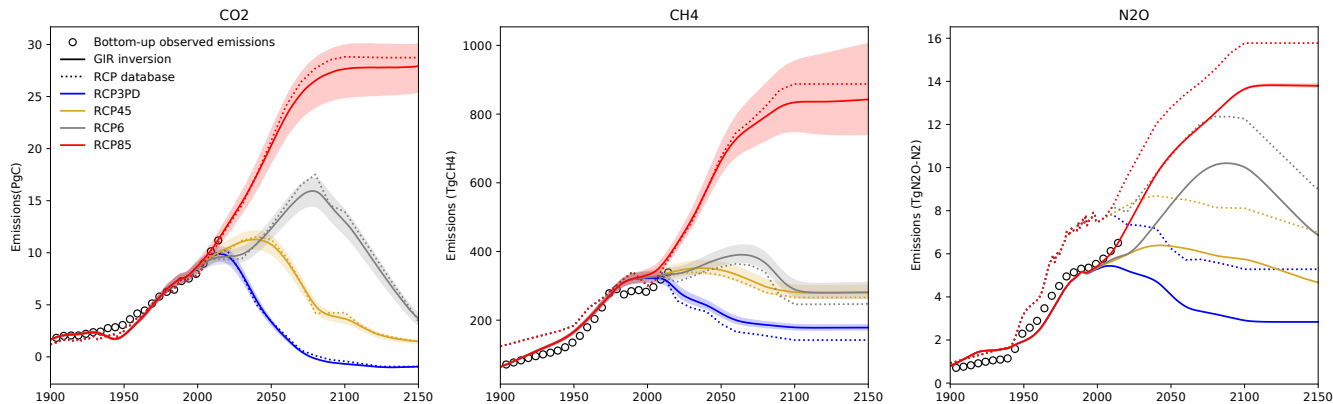
Figure 5. Diagnosed emissions corresponding to the RCPs. Solid lines show best-estimate GIR diagnosed inverse emissions, with associated 5-95% plumes. Dotted lines show emissions directly from the RCP database. Unfilled black circles show bottom-up emission estimates from GCP and PRIMAP-histTP (Quéré et al., 2018; Gütschow et al., 2016), smoothed with a 5-yearly running mean.

1 RCP simulations

This section includes plots of GIR response to the Representative Concentration Pathways; as their use has been widespread in model intercomparisons. Since the RCPs themselves are *concentration* pathways, here we focus on the results of running GIR with concentrations from the RCP database, as was done in the GCMs in CMIP5. Figure 8 shows concentrations resulting from driving GIR with the RCP emissions, demonstrating the incompatibilities between RCP concentrations and emissions due to the lack of integration as was planned in Moss et al. (2010). Figure 5 shows diagnosed emissions that are compatible with the RCP concentration series in GIR, run with default parameters plus uncertainties as described above. Here we see the large discrepancies between GIR compatible emissions and the RCP database emissions for CH_4 and N_2O, while GIR diagnosed emissions agree well with bottom-up emission estimates to the present-day as expected, since GIR is tuned against a very similar historical concentration series; though here we run GIR with the CH_4 r_0 parameter tuned to the Global Methane Budget (Saunois et al., 2019), hence the slight discrepancy between GIR and PRIMAP-histTP.
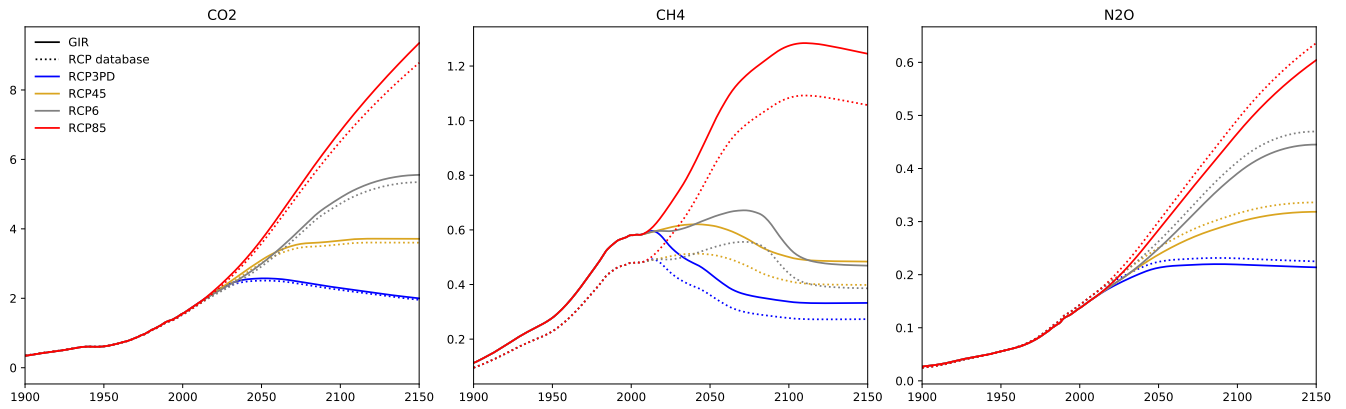
Figure 6. Radiative forcing as computed from the RCP database concentrations using GIR, and corresponding forcings diagnosed by MAG-ICC from the database.

Figure 6 shows the corresponding radiative forcings compared to those from the RCP database. The updated simple RF formulae described in Etminan et al. (2016) increase the RF of CH_4 and CO_2, while marginally decreasing the N_2O RF.
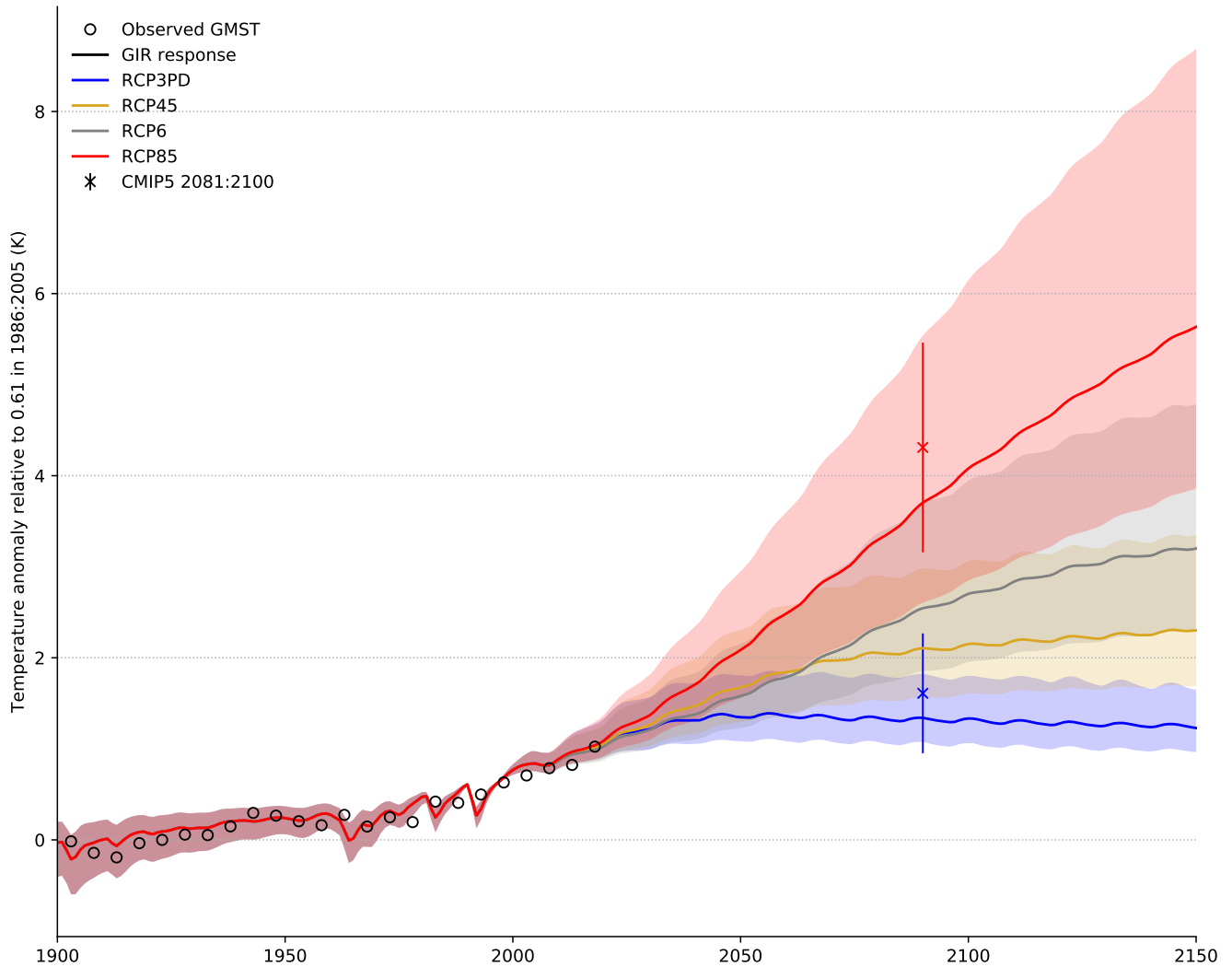
Figure 7. RCP temperature anomalies computed by GIR, and ranges from the CMIP5 ensemble. Solid lines and plumes show best-estimate and 5-95% range temperature anomaly simulated in GIR. Unfilled black circles show observed GMST as the mean of 4 temperature datasets (Vose et al., 2012; Cowtan and Way, 2014; Lenssen et al., 2019; Morice et al., 2011), smoothed with a 5-yearly running mean. Error bars in 2090 show CMIP5 projected 2081:2100 mean temperature anomalies (Collins et al., 2013).

Figure 7 shows historical and future global mean surface temperature ranges (GMST) under the RCP scenarios diagnosed by GIR, alongside historical observed data and future projections from CMIP5. We see that the GIR diagnosed temperatures closely resemble the observed GMST series, but are lower than the CMIP5 ranges. This is due to the default climate response parameter selection in GIR as described above and is discussed in Richardson et al. (2016).
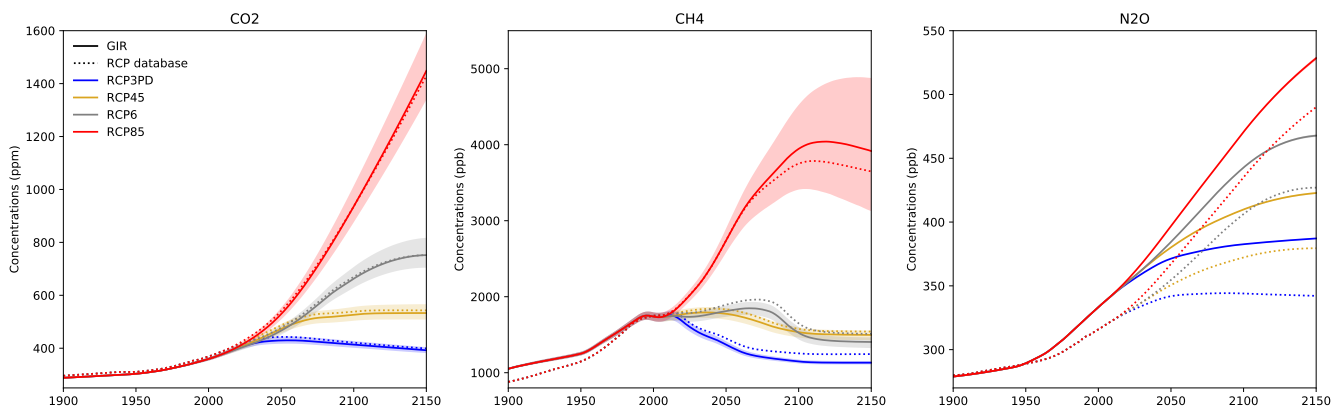
Figure 8. Simulated concentrations when RCP database emissions and other forcings drive GIR, compared to original RCPs. This highlights the historical and future problems of compatibility between the RCP emission and concentration timeseries, especially for N_2O. This issue is discussed more fully in the "Specification of natural emissions" section in the main text.

Code and data availability. The model and code used to produce the figures is publicly available at https://github.com/njleach/GIR, and will

20   be cleaned up and release ready prior to acceptance. All data used in this study is publicly available at the relevant cited sources.

References

Collins, M., Knutti, R., Arblaster, J., Dufresne, J.-L., Fichefet, T., Friedlingstein, P., Gao, X., Gutowski, W. J., Johns, T., Krinner, G., Shongwe, M., Tebaldi, C., Weaver, A. J., and Wehner, M.: Long-term Climate Change: Projections, Commitments and Irreversibility, in: Climate Change 2013: The Physical Science Basis. Contribution of Working Group I to the Fifth Assessment Report of the Intergovernmental Panel on Climate Change, edited by Stocker, T. F., Qin, D., Plattner, G.-K., Tignor, M., Allen, S. K., Boschung, J., Nauels, A., Xia, Y., Bex, V., and Midgley, P. M., chap. 12, pp. 1029–1136, Cambridge University Press, Cambridge, United Kingdom and New York, NY, USA, https://doi.org/10.1017/CBO9781107415324.024, http://www.climatechange2013.org, 2013.

Cowtan, K. and Way, R. G.: Coverage bias in the HadCRUT4 temperature series and its impact on recent temperature trends, Quarterly Journal of the Royal Meteorological Society, 140, 1935–1944, https://doi.org/10.1002/qj.2297, http://doi.wiley.com/10.1002/qj.2297, 2014.

Cunnold, D. M., Fraser, P. J., Weiss, R. F., Prinn, R. G., Simmonds, P. G., Miller, B. R., Alyea, F. N., and Crawford, A. J.: Global trends and annual releases of CCl 3 F and CCl 2 F 2 estimated from ALE/GAGE and other measurements from July 1978 to June 1991 , Journal of Geophysical Research, 99, 1107, https://doi.org/10.1029/93jd02715, 1994.

Etminan, M., Myhre, G., Highwood, E. J., and Shine, K. P.: Radiative forcing of carbon dioxide, methane, and nitrous oxide: A significant revision of the methane radiative forcing, Geophysical Research Letters, 43, 12,614–12,623, https://doi.org/10.1002/2016GL071930, http://doi.wiley.com/10.1002/2016GL071930, 2016.

Gütschow, J., Jeffery, M. L., Gieseke, R., Gebel, R., Stevens, D., Krapp, M., and Rocha, M.: The PRIMAP-hist national historical emissions time series, Earth System Science Data, 8, 571–603, https://doi.org/10.5194/essd-8-571-2016, https://www.earth-syst-sci-data.net/8/571/2016/, 2016.

Lenssen, N. J. L., Schmidt, G. A., Hansen, J. E., Menne, M. J., Persin, A., Ruedy, R., and Zyss, D.: Improvements in the uncertainty model in the Goddard Institute for Space Studies Surface Temperature (GISTEMP) analysis, Journal of Geophysical Research: Atmospheres, p. 2018JD029522, https://doi.org/10.1029/2018JD029522, https://onlinelibrary.wiley.com/doi/abs/10.1029/2018JD029522, 2019.

Millar, R. J., Nicholls, Z. R., Friedlingstein, P., and Allen, M. R.: A modified impulse-response representation of the global near-surface air temperature and atmospheric concentration response to carbon dioxide emissions, Atmospheric Chemistry and Physics, 17, 7213–7228, https://doi.org/10.5194/acp-17-7213-2017, https://www.atmos-chem-phys.net/17/7213/2017/, 2017.

Morice, C. P., Kennedy, J. J., Rayner, N. A., Jones, P. D., P., M. C., J., K. J., A., R. N., and D., J. P.: Quantifying uncertainties in global and regional temperature change using an ensemble of observational estimates: The HadCRUT4 data set, Journal of Geophysical Research: Atmospheres, 117, https://doi.org/10.1029/2011JD017187, https://agupubs.onlinelibrary.wiley.com/doi/abs/10.1029/2011JD017187https://www.metoffice.gov.uk/hadobs/hadcrut4/HadCRUT4{_}accepted.pdf, 2011.

Moss, R. H., Edmonds, J. A., Hibbard, K. A., Manning, M. R., Rose, S. K., Van Vuuren, D. P., Carter, T. R., Emori, S., Kainuma, M., Kram, T., Meehl, G. A., Mitchell, J. F. B., Nakicenovic, N., Riahi, K., Smith, S. J., Stouffer, R. J., Thomson, A. M., Weyant, J. P., and Wilbanks, T. J.: The next generation of scenarios for climate change research and assessment, Nature, 463, https://doi.org/10.1038/nature08823, 2010.

Quéré, C., Andrew, R., Friedlingstein, P., Sitch, S., Hauck, J., Pongratz, J., Pickers, P., Ivar Korsbakken, J., Peters, G., Canadell, J., Arneth, A., Arora, V., Barbero, L., Bastos, A., Bopp, L., Ciais, P., Chini, L., Ciais, P., Doney, S., Gkritzalis, T., Goll, D., Harris, I., Haverd, V., Hoffman, F., Hoppema, M., Houghton, R., Hurtt, G., Ilyina, T., Jain, A., Johannessen, T., Jones, C., Kato, E., Keeling, R., Klein Goldewijk, K., Landschützer, P., Lefèvre, N., Lienert, S., Liu, Z., Lombardozzi, D., Metzl, N., Munro, D., Nabel, J., Nakaoka, S. I., Neill, C., Olsen, A., Ono, T., Patra, P., Peregon, A., Peters, W., Peylin, P., Pfeil, B., Pierrot, D., Poulter, B., Rehder, G., Resplandy, L., Robertson, E.,

Rocher, M., Rödenbeck, C., Schuster, U., Skjelvan, I., Séférian, R., Skjelvan, I., Steinhoff, T., Sutton, A., Tans, P., Tian, H., Tilbrook, B., Tubiello, F., Van Der Laan-Luijkx, I., Van Der Werf, G., Viovy, N., Walker, A., Wiltshire, A., Wright, R., Zaehle, S., and Zheng, B.: Global Carbon Budget 2018, Earth System Science Data, 10, 2141–2194, https://doi.org/10.5194/essd-10-2141-2018, 2018.

Richardson, M., Cowtan, K., Hawkins, E., and Stolpe, M. B.: Reconciled climate response estimates from climate models and the energy budget of Earth, Nature Climate Change, 6, 931–935, https://doi.org/10.1038/nclimate3066, 2016.

Rigby, M., Prinn, R. G., O'Doherty, S., Miller, B. R., Ivy, D., Mühle, J., Harth, C. M., Salameh, P. K., Arnold, T., Weiss, R. F., Krummel, P. B., Steele, L. P., Fraser, P. J., Young, D., and Simmonds, P. G.: Recent and future trends in synthetic greenhouse gas radiative forcing, Geophysical Research Letters, https://doi.org/10.1002/2013GL059099, 2014.

Saunois, M., Stavert, A. R., Poulter, B., Bousquet, P., Canadell, J. G., Jackson, R. B., Raymond, P. A., Dlugokencky, E. J., Houweling, S., Patra, P. K., Ciais, P., Arora, V. K., Bastviken, D., Bergamaschi, P., Blake, D. R., Brailsford, G., Carlson, K. M., Parker, R. J., Peng, C., Peng, S., Peters, G. P., Prigent, C., Prinn, R., Ramonet, M., Regnier, P., Riley, W. J., Rosentreter, J. A., Segers, A., Simpson, I. J., Shi, H., Smith, S. J., Steele, P. L., Thornton, B. F., Tian, H., Tohjima, Y., Tubiello, F. N., Tsuruta, A., Viovy, N., Voulgarakis, A., Weber, T. S., van Weele, M., van der Werf, G. R., Weiss, F., Worthy, D., Wunch, D., Yin, Y., Yoshida, Y., Zhang, W., Zhang, Z., Zhao, Y., Zheng, B., Zhu, Q., Zhu, Q., and Zhuang, Q.: The Global Methane Budget 2000-2017 Earth System Science Data Discussions, Earth System Science Data, https://doi.org/10.5194/essd-2019-128, https://doi.org/10.5194/essd-2019-128, 2019.

Smith, C. J., Forster, P. M., Allen, M., Leach, N., Millar, R. J., Passerello, G. A., and Regayre, L. A.: FAIR v1.1: A simple emissions-based impulse response and carbon cycle model, Geoscientific Model Development Discussions, pp. 1–45, https://doi.org/10.5194/gmd-2017-266, https://www.geosci-model-dev-discuss.net/gmd-2017-266/, 2017.

Vose, R. S., Arndt, D., Banzon, V. F., Easterling, D. R., Gleason, B., Huang, B., Kearns, E., Lawrimore, J. H., Menne, M. J., Peterson, T. C., Reynolds, R. W., Smith, T. M., Williams, C. N., Wuertz, D. B., Vose, R. S., Arndt, D., Banzon, V. F., Easterling, D. R., Gleason, B., Huang, B., Kearns, E., Lawrimore, J. H., Menne, M. J., Peterson, T. C., Reynolds, R. W., Smith, T. M., Jr., C. N. W., and Wuertz, D. B.: NOAA's Merged Land–Ocean Surface Temperature Analysis, Bulletin of the American Meteorological Society, 93, 1677–1685, https://doi.org/10.1175/BAMS-D-11-00241.1, http://journals.ametsoc.org/doi/abs/10.1175/BAMS-D-11-00241.1, 2012.